



ELSEVIER

Available online at www.sciencedirect.com

SCIENCE @ DIRECT®

**NUCLEAR
INSTRUMENTS
& METHODS
IN PHYSICS
RESEARCH**
Section A

Nuclear Instruments and Methods in Physics Research A 544 (2005) 277–284

www.elsevier.com/locate/nima

Ultra-low emittance, high current proton beams produced with a laser-virtual cathode sheath accelerator

T.E. Cowan^{a,i,*}, J. Fuchs^{a,b,i}, H. Ruhl^{a,i}, Y. Sentoku^{a,i}, A. Kemp^{a,i}, P. Audebert^b, M. Roth^c, R. Stephens^a, I. Barton^a, A. Blazevic^c, E. Brambrink^c, J. Cobble^d, J.C. Fernández^d, J.-C. Gauthier^b, M. Geissel^c, M. Hegelich^c, J. Kaae^a, S. Karsch^e, G.P. Le Sage^f, S. Letzring^d, M. Manclossi^g, S. Meyroneinc^h, A. Newkirk^a, H. Pépin^b, N. Renard-LeGalloudecⁱ

^aGeneral Atomics, San Diego, CA 92121, USA

^bLaboratoire pour l'Utilisation des Lasers Intenses, UMR 7605 CNRS-CEA, École Polytechnique, Université Paris VI, 91128 Palaiseau, France

^cGesellschaft für Schwerionenforschung, 64291 Darmstadt, Germany

^dUniversity of California, Los Alamos National Laboratory, Los Alamos, NM 87545, USA

^eMax-Planck-Institut für Quantenoptik, Garching, Germany

^fUniversity of California, Lawrence Livermore National Laboratory, Livermore, CA 94550, USA

^gLaboratoire d'Optique Appliquée, ENSTA - École Polytechnique, 91761 Palaiseau, Cedex, France

^hCentre de Protonthérapie d'Orsay, 91402 Orsay, France

ⁱPhysics Department, MS-220, University of Nevada, Reno, NV 89557, USA

Abstract

The laminarity of high current multi-MeV proton beams produced by irradiating thin metallic foils with ultra-intense lasers has been measured. For proton energies > 10 MeV, the transverse and longitudinal emittance are, respectively, < 0.004 mm mrad and $< 10^{-4}$ eV s, i.e. at least 100-fold and may be as much as 10^4 -fold better than conventional accelerators beams. The ion beam source size is measured to be $< 15 \mu\text{m}$ (fwhm) for proton energies > 10 MeV. Magnetic stripping of the co-moving electrons out of the beam after a few cm of debunching is not observed to induce emittance growth.

© 2005 Elsevier B.V. All rights reserved.

PACS: 52.38.Kd; 29.27.Fh; 52.40.Kh; 52.70.Nc

Keywords: High current proton beams

*Corresponding author. Physics Department, MS-220, University of Nevada, Reno, NV 89557, USA.
E-mail address: cowan@physics.unr.edu (T.E. Cowan).

1. Introduction

The generation of high current multi-MeV protons and ions by irradiating thin foils with short-pulse, ultra-high intensity lasers ($\tau < \text{ps}$, $I\lambda^2 > 10^{18} \text{ W cm}^{-2} \mu\text{m}^2$) [1–6] is a promising new area of research and has renewed speculation for applications like table-top ion accelerators [7,8], high-resolution charged-particle radiography [9], or production of high-energy density matter [10]. The interest in these ion beams lies in their potential high degree of laminarity and extremely low source size.

Our present understanding is that the high laminarity, or low emittance, of these beams stems from the fact the acceleration process takes place on the cold rear (i.e. non-irradiated) surface of the thin foils. There, a dense relativistic electron sheath is formed by the laser-accelerated electrons [1–11] that have propagated through the foil, as illustrated in Fig. 1. This sheath produces an electrostatic field $> 10^{12} \text{ V/m}$ [12] that ionizes the surface atoms almost instantaneously, forming a $\sim 1 \text{ nm}$ thick ion layer which, together with the

electron sheath, resembles a virtual cathode (see Fig. 1). Other mechanisms illustrated in Fig. 1 also produce forward-accelerated ions, although at lower energies and in lower numbers. The resulting accelerated ion beam is composed mostly of protons originating primarily from contaminant layers of water vapor and hydrocarbons on the target surface [4,5]. The extremely strong, transient acceleration that takes place from a cold, initially unperturbed surface, results in the low beam-emittance that seem to be limited only by the collisions with the co-moving electrons during the acceleration [13]. Such an acceleration process represents a new and potentially near-ideal, kind of ion diode as compared either to the ion beams generated from plasma plumes [14], i.e. from the laser-heated turbulent plasma on the front side of the foils, or to the conventional plasma discharge ion sources used in accelerators.

Attempts have been made to measure the beam emittance or source size by using projection, on a far distant film, of objects like knife-edge [15] or meshes [16] placed in the ion beam path. The transverse emittance was estimated to be

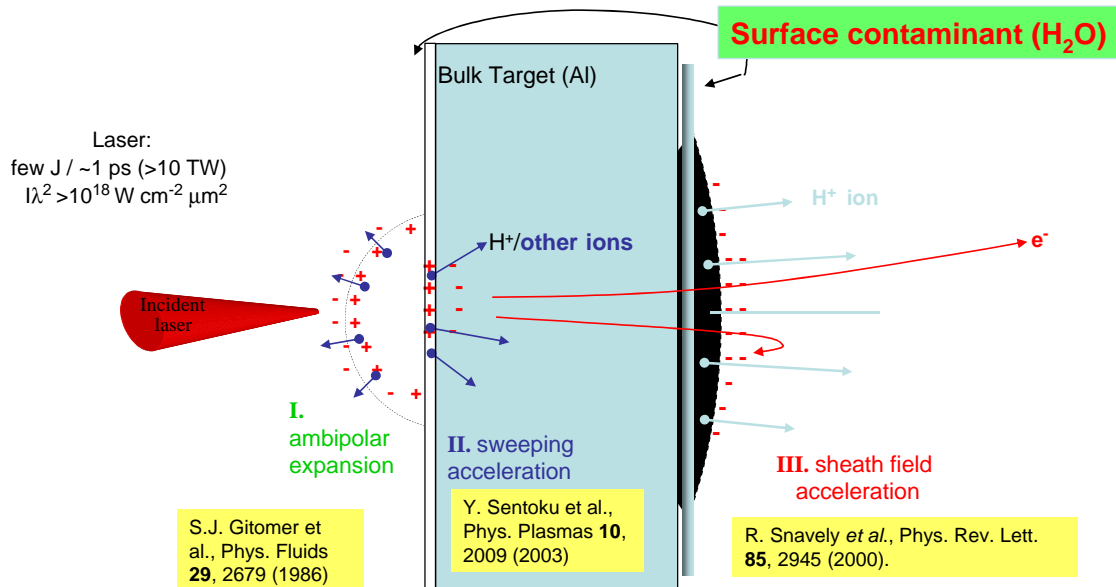


Fig. 1. Principle of the three main mechanisms of laser-acceleration of ions. Ions can be accelerated backwards by the ambi-polar field at the front of laser-irradiated plasma plume. They can be also accelerated forward either by the charge-separation field that is set at the critical density surface or by the sheath field that is set on the target rear-surface. Sheath-field acceleration is found to be largely dominant in our conditions.

= 0.5 mm mrad [15]. However, the ion beam does not propagate ballistically close to the target and passage of the beam on the object induces charge-up that deflects the beam. Therefore, the beam emittance or source size cannot be reconstructed precisely from such measurements.

To overcome these limitations, we have used a new technique that allows to directly image the initial accelerating sheath and to fully reconstruct the transverse phase space [17]. We experimentally show that for protons of up to 10 MeV, the transverse emittance is as low as 0.004 mm mrad, i.e. 100-fold better than typical RF accelerators and at a substantially higher ion current (kA range). In addition, we show that the removal of the co-moving electrons after 2 cm of beam expansion does not increase significantly the measured proton transverse emittance. Simulations also predict a longitudinal phase-space energy–time product 10^5 times better than present proton accelerators. This is the first demonstration of high-current laser-produced charged particle beams with characteristics substantially superior to conventional accelerators. Also, we determine directly for the first time the size of the ion source, a crucial parameter for potential developments of high-resolution charged-particle radiography or ion patterned lithography.

2. Results

The technique we developed for imaging the accelerating sheath uses target design that allows manipulating the ion beam generation during the initial, virtual-cathode phase of the acceleration by generating a stream of beamlets, within the expanding proton envelope, that can be used as fiducials of the acceleration.

The laminarity of charged-particle beams is characterized by their emittance [18], which is proportional to the volume of the bounding ellipsoid of the distribution of particles in phase space. By Liouville’s theorem, the phase-space volume of a particle ensemble is conserved during non-dissipative acceleration and focusing. For the transverse phase-space dimensions (here $x-p_x$ for beam propagation along z), the area of the

bounding phase-space ellipse equals $\pi\varepsilon_N$, where the root-mean-square (rms) value of the “normalized emittance” ε_N at a specific beam energy (or momentum p), is expressed as $\varepsilon_N = (|P|/mc)[\langle x^2 \rangle \langle x'^2 \rangle - \langle xx' \rangle^2]^{1/2}$ where m is the ion mass, c is the velocity of light, x is the particle position within the beam envelope and $x' = p_x/p_z$ is the particles’ divergence in the x -direction. At a beam waist, $\varepsilon_N = \beta\gamma\sigma_x\sigma_{x'}$ where σ_x and $\sigma_{x'}$ are the rms values of the beam width and divergence angle. For typical proton accelerators (e.g., the CERN SPS), the emittance from the proton injector linac is ~ 1 mm mrad (normalized-rms) and up to 3.5 mm mrad within the synchrotron, with 10^{11} protons per bunch. The longitudinal phase-space ($z-p_z$) is characterized by the equivalent, energy–time product of the beam envelope and a typical value, for the CERN SPS, is ~ 0.5 eV s. The highest quality ion beams have the lowest values of transverse and longitudinal emittance, indicating a low effective transverse ion temperature and a high degree of angle-space and time–energy correlation.

We have assessed the characteristics of the laser-accelerated ion beams in experiments performed using the 100 TW short pulse laser system at the Laboratoire pour l’Utilisation des Lasers Intenses (LULI), and the 30 TW Trident laser at the Los Alamos National Laboratory. The concept of the experiment is shown schematically in Fig. 1. Laser pulses of ~ 20 – 30 J of $1\ \mu\text{m}$ light (350–850 fs) were focused onto the front surface of thin foils of Au or Al (10–50 μm thick). Note that the targets can only be used once since they are destroyed during the shot. The accelerated protons are detected in multiple layers of radiochromic film (RCF) densitometry media [19]. The spatial distribution of the protons in a given RCF layer gives the angular emission pattern at a specific interval of proton energy. By carefully preparing the rear surface of the target foil, and by shaping the laser focal intensity distribution, we controlled the virtual-cathode phase of the acceleration where the electric field is normal to the ion charge layer [11,20]. For the data of Fig. 2a–c, we used optically flat aluminum foils on the rear surface of which we micro-machined shallow grooves, 200 nm deep spaced $3.6\ \mu\text{m}$ apart. The grooves

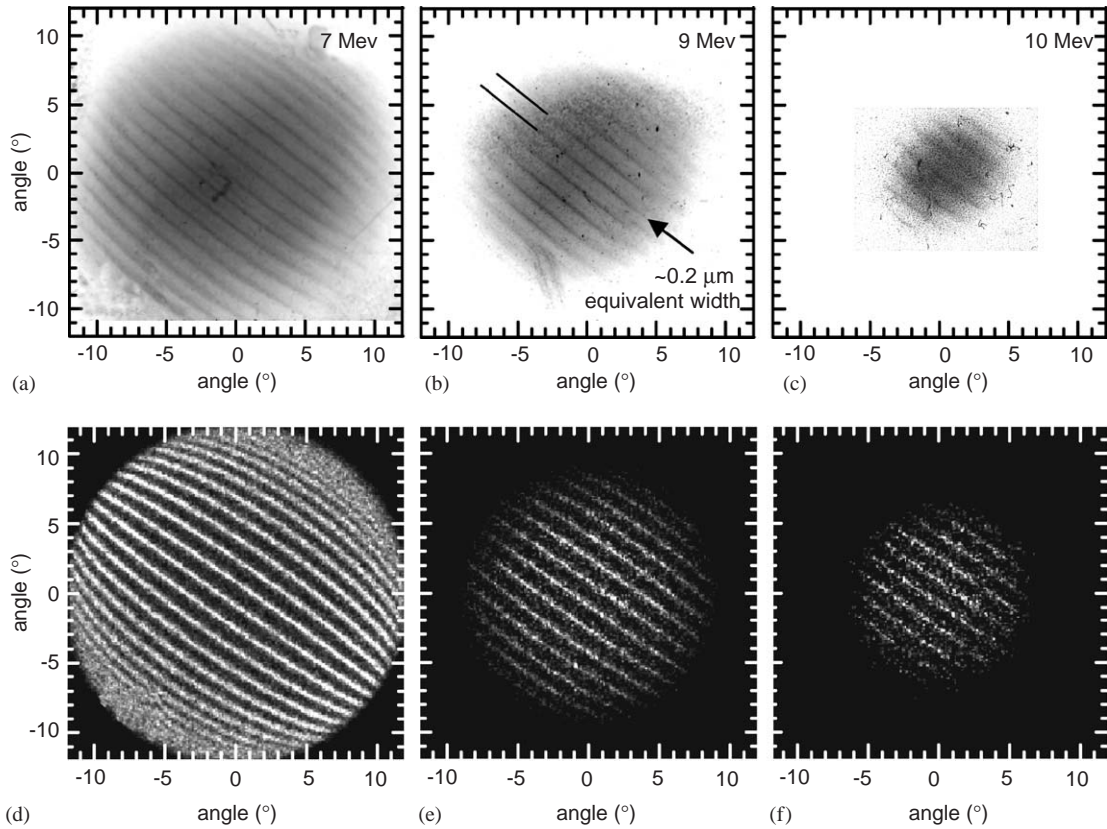


Fig. 2. (a–c) Spatial distributions at different energies of protons accelerated from a 18 μm thick Al flat target irradiated at 10^{19} W/cm² and detected on the RCF film stack placed 68 mm from the target. Micro-focused beam-fiducials map the emission zone at the virtual cathode, which decreases at higher proton energy. (d–f) Corresponding simulated RCF images (same parameters and proton energies as in a–c) using a 3D PIC effective code with an assumed transverse proton temperature of 100 eV.

appear to electrostatically focus the protons near the target surface to individual beamlets, ~ 200 nm wide (rms), during this first phase, after which the expanding sheath produces a correlation between the initial source position and final divergence angle [11,20]. The proton angular distributions at mean energies of 7, 9 and 10 MeV are shown in Fig. 2a–c. From a quantitative analysis of the film optical densities, we measure that $\sim 10^{11}$ protons are produced in a single laser-shot for energies above 4 MeV, which corresponds to an ion current of > 1 kA at 1 mm from the target foil. The proton energy distribution decreases as $dN/dE \propto \exp(-E/[2.6 \text{ MeV}])$. We also observe a decrease in the angular envelope of the protons with increasing

proton energy, as has been observed before [4,5]. However, using the modulation of the beam intensity impressed during the initial phase, we are able to image the proton-emitting surface and thus to measure for the first time directly the source size. By accelerating protons off non-periodic surface structures, we verified that there is no overlap of the beam fiducials from adjacent structures that could lead to misinterpretation of the data. We establish that for protons above 4.5 MeV, the decrease in the angular envelope with energy is due to a decrease of the emitting zone, but not due to a strong change in the divergence (i.e., magnification) of the beam envelope or from magnetic field deflection [2,21].

Such a decrease of the emission zone is expected for a transversally bell-shaped electron density distribution. In such a sheath, the highest energy protons are accelerated in the central, high-density portion of the sheath, whereas lower energies come from the wings of the sheath distribution and thus are emitted at larger angle [20]. The measured diameter of the virtual-cathode emission zone is of

order of $50\ \mu\text{m}$ (fwhm) at $4.5\ \text{MeV}$, and $\sim 30\ \mu\text{m}$ (fwhm) for $>9\ \text{MeV}$ protons.

In Fig. 3a, we plot the divergence angle vs. the source position of the accelerated protons by using the nano-focused structures as fiducial marks impressed in the initial beam. Note that within the central portion of the beam the phase-space correlation is almost exactly linear. This remark-

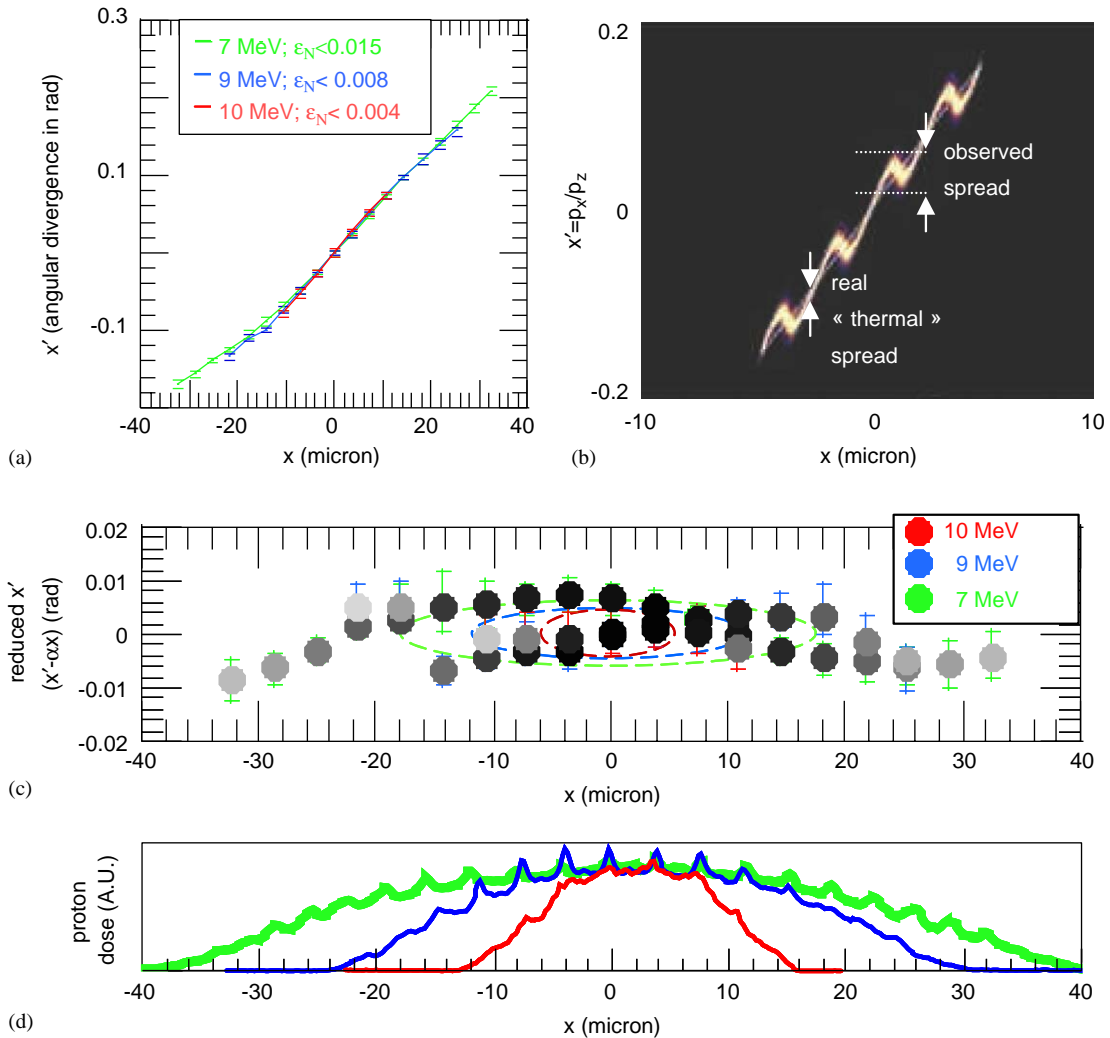


Fig. 3. (a) Transverse phase-space plot the proton beam (from Fig. 2a–c). Error flags denote the rms angular width (1σ) of the beamlets. This gives an upper limit on envelope divergence, from which we estimate an upper limit of the emittance ϵ_N at each energy, as marked (in units mm mrad). (b) Same from the effective PIC simulation 600 fs after the interaction. (c) Same as (a) but in a rotated frame. The emittance ellipses using the Twiss parameters are overlaid. The transparencies of the dots encode the value of the dose at each point, following the curves shown in (d).

able result suggests that the relativistic electron sheath has a nearly Gaussian-radial distribution in its density profile, which gives a nearly linear relation between radial position and the radial electric field in the sheath. Note that this is supported by the 3D PIC simulation which displays the same behavior as shown in Fig. 3b.

By assuming that the protons in each beamlet come from an ideal line focus, we experimentally deduce an upper limit on the transverse emittance of <0.004 mm mrad for 10 MeV protons, a factor of >100 smaller than typical proton beam sources. We attribute this to the fact that during much of the acceleration the proton space charge is neutralized by the co-moving hot electrons, and that the sheath electric field self-consistently evolves with the ions to produce an effectively “ideal” accelerating structure. PIC simulations show that the image generation is more complicated. Indeed, as shown in Fig. 3b, the observed angular width of the beamlets, which is a projection in $x' = p_x/p_z$ of the transverse phase space, involves the magnitude of the initial transverse momentum oscillation in addition to the irreducible thermal spread.

Accordingly, the actual transverse emittance could be smaller than the deduced <0.004 mm mrad. The irreducible “thermal” contribution to the emittance can be interpreted as an effective proton transverse Maxwellian temperature ranging from <15 eV for the highest resolution portion of the data, to <200 eV at the edge of the beam. The reconstructed RCF images in Fig. 2d–f assumed a transverse proton temperature of 100 eV, which is consistent with the data but appears to overestimate the width of the highest resolution beamlets. Separate 1D PIC simulations that include binary collisions show a ratio of longitudinal to transverse ion temperature of $\sim 10^5$ – 10^6 for sheath-accelerated ions of ~ 10 MeV [13], in agreement with the experimental results. Without collisions, the simulation does not exhibit any transverse ion temperature. This suggests that an ideal collisionless acceleration would produce a perfectly laminar beam but the collisional heating of the ions during the early virtual cathode stage will set the absolute limit on the achievable emittance.

The energy spread of the laser-accelerated proton beam is large, ranging from 0–10 MeV,

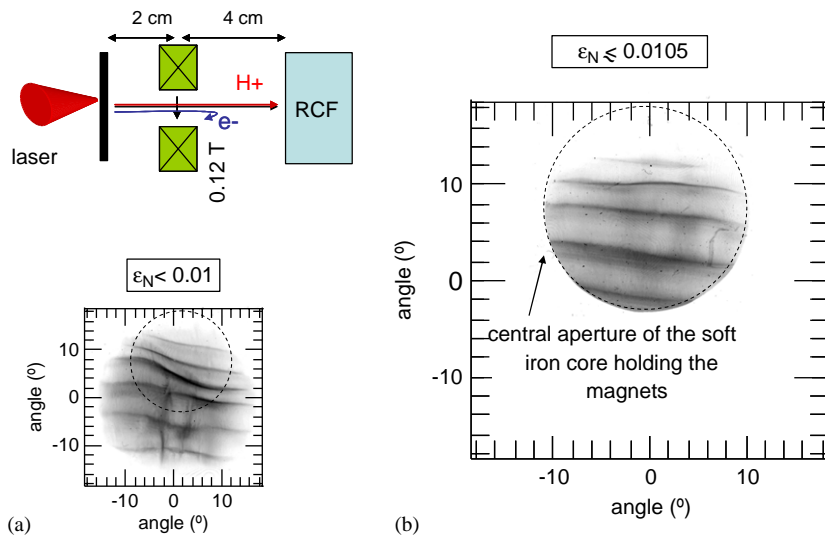


Fig. 4. (a) Schematic representation of the electron stripping experiment. A dipole magnet is positioned downstream from the source foil irradiated by the laser. Electrons are confined by oscillations in the magnetic field. (b) Structured ion part at ~ 6.5 MeV of the neutralized beam produced by a 10^{19} W/cm² pulse incident on a $40 \mu\text{m}$ thick Al foil. Observed ripples in the laser focal spot that can deform the bell-shaped sheath [20] are likely to induce the observed distortions in the beam; the RCF is placed 59 mm from the target, (b) non-neutral ion part of the beam; a 0.12 T magnet placed 20 mm behind the target ensures that all electrons are separated from the ions within a few mm. The measured emittance represents an effective proton source transverse Maxwellian temperature of 125 eV.

however due to the extremely short duration of the accelerating field (<10 ps), the longitudinal phase-space energy–time product must be less than 10^{-4} eVs. The 3D PIC simulations show that longitudinally the acceleration is extremely laminar, in the sense that the spread of proton energies in a given longitudinal slice is very

small. We estimate from the simulation an energy–time product of $<10^{-7}$ eVs. Such extremely good longitudinal velocity “chirp” of the beam is interesting since it could in principle allow to monochromatize a portion of the beam by coupling it to the field gradient of a post-accelerator.

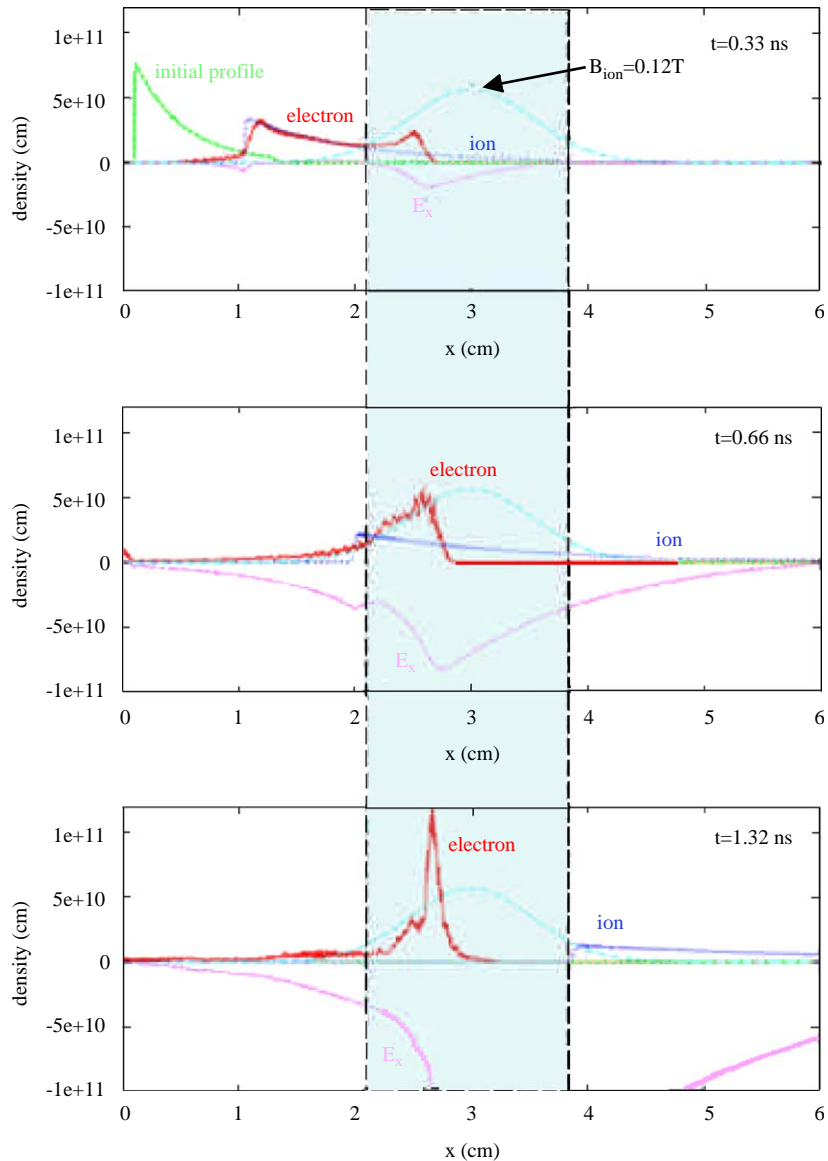


Fig. 5. 1D PIC simulation of co-moving electrons stripping out of the plasma beam by a 0.12 T magnetic field positioned downstream from the target foil where the beam (electrons + protons) is accelerated. The beam density and the particles energies are deduced from experimental measurements. The magnetic pressure, far greater than the space-charge one, ensures the removal of the electrons.

In order to take advantage of the exceptionally small proton beam emittance in future applications, e.g. to focus the ions or to capture them into a post-accelerator, removal of the co-moving electrons without significantly perturbing the protons is important. We tested if this could be done without increasing the transverse temperature of the beam. As shown in Fig. 4, we compared the situation where the neutralized plasma beam expands freely up to the RCF detector; or where we placed a pair of magnets 2 cm downstream from the target to remove all the electrons from the beam and let the non-neutral ion beam propagate 4 cm further to the RCF. A global increase of the ion beam envelope is expected for the non-neutral beam but no significant difference in the inferred emittance can be seen between the two shots. It shows that at this stage the removal, by the external B-field, of the electrons that allowed the beam to accelerate laminarly, does not increase the ion transverse temperature, such as might occur from turbulence in the electron trajectories resulting from the ion-induced space-charge and the B-field. Complementary measurement [22] show that the electron temperatures are <100 eV at the time they reach the magnet, with energies of a few keV, i.e. the electrons are essentially co-moving with the protons. We checked, using PIC simulations, as shown in Fig. 5, that the magnet was effective in removing the electrons from the neutral plasma beam.

The potential impact of ultra-low emittance, high-current laser-driven proton beams for accelerator physics could be significant. If the low transverse emittance could be maintained throughout the accelerator and up to the collision point of a high-energy physics (HEP) machine, it would directly increase the luminosity and hence the discovery potential of existing facilities [23]. Such photo-hadron sources may impact the low-energy booster section of HEP accelerators, by allowing smaller apertures and a higher bunch charge. Capture and post-acceleration of such beams may also enable compact accelerators that could lead to a wider use of hadron beams for cancer therapy [24,25]. Finally, the beam laminarity is the enabling factor that could lead to significant progress in other applications, e.g., for

radiography [9], generation of complex patterned beams, and for ion focusing to produce and/or probe high energy density matter and for fusion by Fast Ignition [10,26].

Acknowledgements

We acknowledge the expert support of the LULI and Trident laser teams, and useful discussions with G. Dugan. This work was supported by Grant E1127 from Région Ile-de-France, EU program HPRI CT 1999-0052, LANL Laboratory Directed Research & Development, corporate support of General Atomics and UNR Grant DE-FC08-01NV14050.

References

- [1] S. Hatchett, et al., *Phys. Plasmas* 7 (2000) 2076.
- [2] E. Clark, et al., *Phys. Rev. Lett.* 84 (2000) 670.
- [3] A. Maksimchuk, et al., *Phys. Rev. Lett.* 84 (2000) 4108.
- [4] R.A. Snavely, et al., *Phys. Rev. Lett.* 85 (2000) 2945.
- [5] M. Roth, et al., *Phys. Rev. ST-AB* 5 (2002) 061301.
- [6] M. Hegelich, et al., *Phys. Rev. Lett.* 89 (2002) 085002.
- [7] D. Habs, et al., *Prog. Part. Nucl. Phys.* 46 (2001) 375.
- [8] I. Spencer, et al., *Nucl. Instrum. and Meth. B* 183 (2001) 449.
- [9] M. Borghesi, et al., *Plasma Phys. Contr. F.* 9 (2001) A267; J.A. Cobble, et al., *J. Appl. Phys.* 92 (2002) 1775.
- [10] P. Patel, et al., *Phys. Rev. Lett.* 91 (2003) 125004.
- [11] H. Ruhl, et al., *Phys. Plasmas* (2004), in press.
- [12] S. Wilks, et al., *Phys. Plasmas* 8 (2000) 532.
- [13] A. Kemp, et al., in preparation.
- [14] S.J. Gitomer, et al., *Phys. Fluids* 29 (1986) 2679.
- [15] T.E. Cowan, et al., Laser generation of accelerator quality proton beams, in: *High Brightness Beams*, World Scientific Press, Singapore, 2000.
- [16] M. Borghesi, et al., *Phys. Rev. Lett.* 92 (2004) 055003.
- [17] T. Cowan, et al., *Phys. Rev. Lett.* 92 (2004) 204801.
- [18] S. Humphries, *Charged Particle Beams*, Wiley, New York, 1990.
- [19] N.V. Klassen, et al., *Med. Phys.* 24 (1997) 1924.
- [20] J. Fuchs, et al., *Phys. Rev. Lett.* 91 (2003) 255002.
- [21] Y. Murakami, et al., *Phys. Plasmas* 8 (2001) 4138.
- [22] M. Cuneo, et al., in preparation.
- [23] W. Chou, in: A. Luccio, W. MacKay (Eds.), *Proceedings of 1999 Particle Accelerator Conference*, IEEE, New York, 1999, p. 3285.
- [24] A.L. Boyer, et al., *Physics Today* 55 (2002) 34.
- [25] E. Fourkal, et al., *Med. Phys.* 29 (2002) 2788.
- [26] M. Roth, et al., *Phys. Rev. Lett.* 86 (2001) 436.